Haptic Data Prediction and Extrapolation for Communication Traffic Reduction of Four-Channel Bilateral Control System

Satoshi Hangai, *Student Member, IEEE*, and Takahiro Nozaki, *Member, IEEE*

***Abstract*—Robotic teleoperation with a bilateral control system has attracted attention owing to its haptic transmission performance. However, conventional bilateral control systems require broadband communication to transmit the vivid haptic sensation. This problem limits the application range of the bilateral control systems. The communication traffic can be reduced by predicting and extrapolating the incoming data. However, in the conventional prediction-based methods, only one type (e.g., position, velocity, or force) of data is transmitted per one direction because of the difficulty of predicting multiple independent data. The novelty of this article is the realization of the prediction-based traffic reduction in the four-channel bilateral control system that transmits accurate haptic sensation by communicating both position and force data. By equivalently transforming this control scheme in the structure of impedance control, the transmit data are summed up to one data, equilibrium force. The equilibrium force is not only transmitted but extrapolated on the receiver side. As a result, the communication frequency becomes low without degrading haptic transmission performance. The validity of the proposed method was confirmed through experiments and succeeded to reduce the communication data size to less than 3.0%. The proposed method helps to realize a high-performance bilateral control system on band-limited networks.**

***Index Terms*—Haptics, bilateral control, teleoperation, traffic reduction, information technology.**

I. Introduction

HAPTIC transmission technologies attract a lot of attention because they assist in improving robotic teleoperation [1]–[3]. Application of haptic information in robotic teleoperation will help operators to manipulate remote objects softly as if they are in remote places. As a result, they can conduct difficult tasks, such as surgery in a remote area. The application range of the haptic transmission technologies will expand with the recent development of wireless network like the fifth generation wireless technology for digital cellular networks [4], [5]. Bilateral control [6]–[9] is one of the key technologies to achieve haptic transmission. The bilateral control system comprises of a master robot and a slave robot. When an operator moves the master robot, the slave robot tracks the master robot's motion. Moreover, when the slave robot contacts with objects, a reaction force is transmitted to the master robot. As a result, the operator can feel the slave side's haptic sensation through the master robot.

A communication traffic reduction is one of the major concerns of the networked bilateral control system. To transmit vivid haptic sensation, communication frequency between the two robots should be high. However, if the communication frequency is too high, the communication data size may exceed the communication channel capacity. Moreover, too high communication frequency can increase the communication time delay [10]. This large communication time delay not only degrades the operationality but also makes the system unstable [11]–[13].

To reduce the communication frequency of the bilateral control system, prediction-based approaches have been proposed [14][15]. These approaches are mainly developed based on human perception [16]–[18]. If the variance in the haptic data is too small for a human to notice, the haptic data are ignored and not transmitted to the receiver side. During this state, the missing haptic data are extrapolated using the previously received data samples. This helps to reduce the packet transmission frequency without deteriorating haptic transmission performance. In a study by [14], the prediction-based approach was implemented to a system, which transmit the position (including the velocity) data as haptic information. In experiments simulating surgical tasks, the amount of transmitted packets were reduced to less than 2.4% while maintaining the haptic transmission performance. However, in the previous prediction-based approaches, only the position or force information can be transmitted from one side to the other side due to the difficulty of predicting the multiple independent signals. These approaches have not been applied to a four-channel bilateral control system that shows high haptic transmission performance by communicating both position and force data bidirectionally [19].

The novelty of this article is to realize the prediction-based traffic reduction in the four-channel bilateral

Manuscript received March 25, 2020; revised May 6, 2020; accepted May 14, 2020. Date of publication May 20, 2020; date of current version January 4, 2021. This work was supported by JSPS KAKENHI under Grant JP20H02135 and Grant JP19KK0367. Paper no. TII-20-1535. *(Corresponding author: Satoshi Hangai.)*

Satoshi Hangai was with the Department of System Design Engineering, Keio University, Yokohama 223-8522, Japan, and is now with Nippon Steel Corporation, Chiba 293-8511, Japan (e-mail: hangai@sum.sd.keio.ac.jp).

Takahiro Nozaki is with the Department of System Design Engineering, Keio University, Yokohama 223-8522, Japan, and also with the Department of Mechanical Engineering, Massachusetts Institute of Technology, Cambridge, MA 02139 USA (e-mail: nozaki@sd.keio.ac.jp).

Color versions of one or more of the figures in this article are available online at https://ieeexplore.ieee.org.

Digital Object Identifier 10.1109/TII.2020.2995627

TABLE I
NOMENCLATURE

Symbols	Definitions
x	Position
f	Force
s	Laplace operator
K_{p}	Positional feedback gain
K_{v}	Velocity feedback gain
K_{f}	Force feedback gain
z	Control impedance
$\bigcirc_{\mathrm{m}}$	Master
$\bigcirc_{\mathrm{s}}$	Slave
$\bigcirc^{\mathrm{cmd}}$	Command value
$\bigcirc^{\mathrm{ref}}$	Reference value
$\bigcirc_{\mathrm{m}\to\mathrm{s}}$	Data transmitted from master to slave
$\bigcirc_{\mathrm{s}\to\mathrm{m}}$	Data transmitted from slave to master

control system. In a study by [20], the conventional four-channel bilateral control system is equivalently transformed into the structure of impedance control. After this transformation, the transmit data (position and force) are summed up to only one data, equilibrium force. This article verifies that communication traffic reduction can be realized by predicting and extrapolating the equilibrium force. In the proposed method, the equilibrium force is not only transmitted but also linear-extrapolated in the receiver side. The equilibrium force is only transmitted when the extrapolation is estimated as difficult. As a result, the communication frequency becomes low without degrading the haptic transmission performance of the four-channel bilateral control system.

The rest of this article is organized as follows: In Section II, we introduce the structure of the four-channel bilateral control system and equivalently transform the control structure in impedance field expression. In Section III, the prediction-based communication traffic reduction is realized in the introduced bilateral control system. Simulations are conducted in Section IV to design and analyze the proposed method. Experiments are performed in Section V. The same experiments are also conducted under the existence of communication time delay. Finally, Section VI concludes this article.

II. Four-Channel Bilateral Control System Based on Impedance Field Expression

The bilateral control system comprises of a master robot and a slave robot. When an operator manipulates the master robot, the slave robot tracks the master robot's motion and touches with environmental objects. The external force from the objects is measured or estimated on the slave side, and fed back to the master robot. Therefore, the operator can feel the external force through the master robot. Symbols shown in the following explanation are listed in Table I.

The bilateral control system has two control goals. The first goal is to synchronize the two robots' position as

$$x_m - x_s = 0. \tag{1}$$

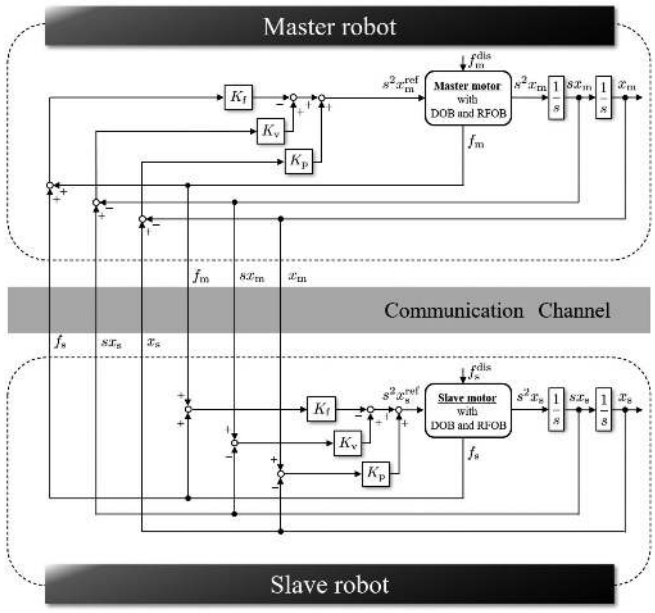

Fig. 1. Block diagram of four-channel bilateral control system. Three types of data are transmitted bidirectionally in the conventional four-channel bilateral control system.

The second goal is to realize the law of action and reaction between the two robots as

$$f_m + f_s = 0. \tag{2}$$

The four-channel bilateral control system [19] is one of the control structures to achieve the above two control goals. Both the position and force information are transmitted bidirectionally in the four-channel bilateral control system. Using the position and force information, the above control goals (1) and (2) are achieved by the position controller and the force controller, respectively. In this article, the four-channel bilateral control system is achieved with the acceleration control. The acceleration references are expressed as

$$s^2 x_m^{\mathrm{ref}} = K_p(x_s - x_m) + K_v(sx_s - sx_m) - K_f(f_m + f_s) \tag{3}$$

$$s^2 x_s^{\mathrm{ref}} = K_p(x_m - x_s) + K_v(sx_m - sx_s) - K_f(f_m + f_s) \tag{4}$$

Fig. 1 shows the block diagram of the four-channel bilateral control system. The above acceleration references are achieved with disturbance observer (DOB) [21]. Moreover, the external force f_m and f_s are estimated by reaction force observer (RFOB) [22]. As shown in Fig. 1, three types of data are transmitted bidirectionally in the conventional four-channel bilateral control system. These multiple data flows make it difficult to apply the prediction-based traffic reduction techniques [14], [15] in the four-channel bilateral control system.

The control structure shown in Fig. 1 can be equivalently transformed to that of impedance control [20]. The acceleration references (3) and (4) are rewritten as

$$s^2 x_m^{\mathrm{ref}} = K_f\left[\left\{f_{s\to m}^{\mathrm{cmd}} - z(sx_m)\right\} - f_m\right] \tag{5}$$

$$s^2 x_s^{\mathrm{ref}} = K_f\left[\left\{f_{m\to s}^{\mathrm{cmd}} - z(sx_s)\right\} - f_s\right] \tag{6}$$

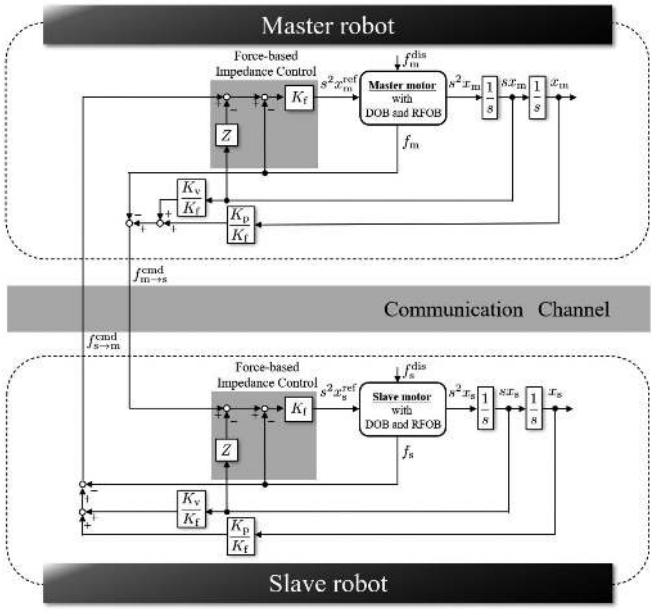

Fig. 2. Impedance field expression of four-channel bilateral control system. The transmit data between the two robots in Fig. 1 are summarized to only one data, the force command that represents the equilibrium force.

where the force commands f^{cmd} and control impedance z are defined as

$$f^{\mathrm{cmd}}_{m\to s} = \frac{K_{\mathrm{p}} + K_{\mathrm{v}} s}{K_f} x_m - f_m \tag{7}$$

$$f^{\mathrm{cmd}}_{s\to m} = \frac{K_{\mathrm{p}} + K_{\mathrm{v}} s}{K_f} x_s - f_s \tag{8}$$

$$z = \frac{1}{s}\frac{K_{\mathrm{p}} + K_{\mathrm{v}} s}{K_f}. \tag{9}$$

As shown in (5) and (6), the control references of the four-channel bilateral control system are expressed in the architecture of force-based impedance control. Fig. 2 shows the block diagram of the bilateral control system based on the impedance field expression. By equivalently transforming Figs. 1–2, the transmit data between the two robots are summarized to only one data, the force command that represents the equilibrium force. Therefore, the communication traffic of the four-channel control system is reduced by applying this equivalent transformation. Moreover, this summarization of the data flow makes it possible to predict the incoming data for traffic reduction, which is discussed in the following sections.

III. Communication Traffic Reduction by Haptic Data Prediction and Extrapolation

In this section, the prediction-based communication traffic reduction is realized in the previously introduced four-channel bilateral control system. Fig. 3(a) shows the entire structure of the proposed method. For simplicity, the equilibrium force transmission from the master side to the slave side is only explained. In the proposed method, the communication frequency is reduced by shifting the two communication modes: the extrapolation mode and the transmission mode. In the extrapolation mode, data transmission is stopped to reduce the communication frequency as shown in Fig. 3(b). Instead, the missing data are extrapolated on the slave side's extrapolator. Data transmission is carried out only in the transmission mode as shown in Fig. 3(c). This mode transition is carried out by the master side's predictor. The detailed explanation of the data extrapolation and the mode transition are shown in Section III-A and III-B, respectively. The time derivative of the equilibrium force is required in the extrapolator and the predictor functions. The time differentiation method of the equilibrium force is explained in Section III-C.

A. Linear-Extrapolation of Missing Equilibrium Force

The slave robot extrapolates the equilibrium force if the packets are not transmitted from the master side. The equilibrium force is linear-extrapolated using the last received equilibrium force and its time derivative as

$$f^{\mathrm{exp}}_s[k] = f^{\mathrm{cmd}}_{m\to s}[k_{\mathrm{T}}] + \sum_{n=1}^{k-k_{\mathrm{R}}} \dot{f}^{\mathrm{cmd}}_{m\to s}[k_{\mathrm{T}}]\delta t \tag{10}$$

where f^{exp}_s, k, and δt denote the extrapolation force, time, and the sampling time, respectively. k_{T} and k_{R} denote the last time when the master controller transmitted data to the slave side, and the last time when the slave robot received data from the master side, respectively. The acceleration reference of the slave robot is expressed as

$$s^2 x^{\mathrm{ref}}_s[k] = K_f\left[\{f^{\mathrm{exp}}_s[k] - z(s x_s[k])\} - f_s[k]\right]. \tag{11}$$

As expressed in (11), the extrapolation force f^{exp}_s substitutes the actual equilibrium force $f^{\mathrm{cmd}}_{m\to s}$ when the data are not transmitted from the master side.

B. Mode Transition for Communication Frequency Reduction

The mode transition is carried out using the output of the predictor. The master side's predictor estimates the slave side's extrapolation force as

$$\begin{aligned}\hat{f}^{\mathrm{exp}}_s[k] &= f^{\mathrm{cmd}}_{m\to s}[k_{\mathrm{T}}] + \sum_{n=1}^{k-k_{\mathrm{T}}} \dot{f}^{\mathrm{cmd}}_{m\to s}[k_{\mathrm{T}}]\delta t \\ &= f^{\mathrm{exp}}_s[k] + \sum_{n=1}^{T/\delta t} \dot{f}^{\mathrm{cmd}}_{m\to s}[k_{\mathrm{T}}]\delta t \\ &= f^{\mathrm{exp}}_s\left[k + \frac{T}{\delta t}\right]\end{aligned} \tag{12}$$

where $\hat{f}^{\mathrm{exp}}_s$ and T represent the prediction value of the extrapolation force on the slave side and communication delay time between the two robots. When the predicted extrapolation force $\hat{f}^{\mathrm{exp}}_s[k]$ is close to the actual equilibrium force $f^{\mathrm{cmd}}_{m\to s}[k]$, the extrapolation is carried out with high accuracy. Therefore, the data are not transmitted to the slave side. The condition of the extrapolation mode is expressed as

$$|f^{\mathrm{cmd}}_{m\to s}[k] - \hat{f}^{\mathrm{exp}}_s[k]| \le f^{\mathrm{error}} \tag{13}$$

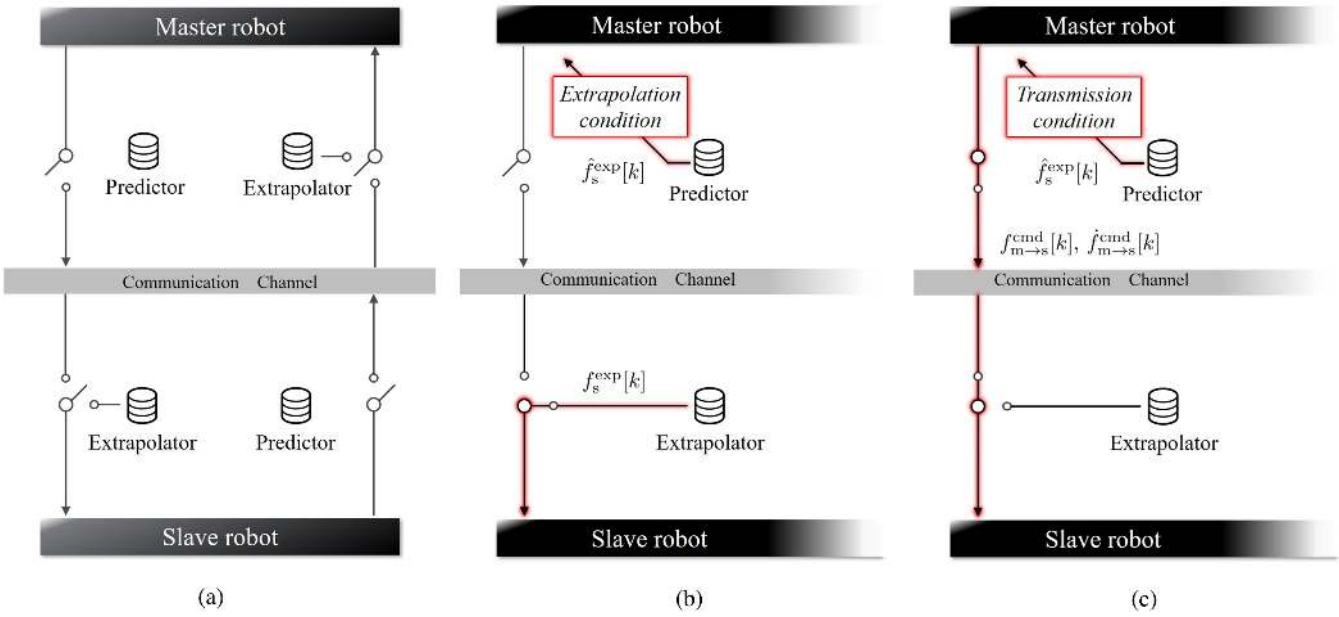

Fig. 3. Communication traffic reduction by haptic data prediction and extrapolation. (a) Entire structure of proposed method. (b) Extrapolation mode. (c) Transmission mode.

where f^{error} means the threshold of the extrapolation error of the equilibrium force. By setting the threshold sufficiently small, the performance and stability are not deteriorated from the conventional four-channel bilateral control system. The situation of the extrapolation mode is shown in Fig. 4(a). On the other hand, the master controller transmits data to the slave side only when (13) is not satisfied as shown in Fig. 4(b).

C. Time Differentiation Method of Equilibrium Force

To carry out a linear-extrapolation of the equilibrium force, both the equilibrium force and its time derivative are transmitted. However, the time derivative of the equilibrium force is badly affected by the sensing noise since the equilibrium force consists of force information as shown in (7) and (8). The force information itself is low-pass filtered in the estimation process by RFOB [22]. To enhance the noise reduction effect in the time-differentiation process of the equilibrium force, a Savitzky–Golay (S–G) [23] filter is implemented.

The S–G filter is one of the digital filters used for data smoothing and differentiation based on the least-squares polynomial approximation [24]–[26]. Moreover, the S–G filter is effective for derivative time series signal owing to its data smoothing function [27].

We approximate the equilibrium force $f_{m\to s}^{\mathrm{cmd}}$ using n_{w} data samples as a first-order function as

$$\hat{f}_{m\to s}^{\mathrm{cmd}}[k+m] = c_0 + c_1(k+m)\delta t \tag{14}$$

where c_0 and c_1 are the coefficients of the approximated function, and m is an integer which satisfies

$$-n_{\mathrm{w}} + 1 \le m \le 0. \tag{15}$$

n_{w} is a window size of the S–G filer that takes an odd value. In vector form, the (14) is expressed as

$$\hat{\boldsymbol{f}} = c_0\boldsymbol{s}_0 + c_1\boldsymbol{s}_1 \tag{16}$$

$$= \boldsymbol{S}\boldsymbol{c} \tag{17}$$

where $\hat{\boldsymbol{f}}$, $\boldsymbol{s}_0$, $\boldsymbol{s}_1$, $\boldsymbol{S}$, and $\boldsymbol{c}$ are expressed as

$$\hat{\boldsymbol{f}} = \left(\hat{f}_{m\to s}^{\mathrm{cmd}}[k-n_{\mathrm{w}}+1],\ \hat{f}_{m\to s}^{\mathrm{cmd}}[k-n_{\mathrm{w}}+2]\right.$$
$$\left.\ldots,\ \hat{f}_{m\to s}^{\mathrm{cmd}}[k-1],\ \hat{f}_{m\to s}^{\mathrm{cmd}}[k]\right)^T \tag{18}$$

$$\boldsymbol{s}_0 = (1,\ 1,\ldots,\ 1)^T \tag{19}$$

$$\boldsymbol{s}_1 = (k-n_{\mathrm{w}}+1,\ k-n_{\mathrm{w}}+2,\ldots,\ k)^T\,\delta t \tag{20}$$

$$\boldsymbol{S} = (\boldsymbol{s}_0,\ \boldsymbol{s}_1) \tag{21}$$

$$\boldsymbol{c} = (c_0,\ c_1)^T. \tag{22}$$

Here, the performance index $\boldsymbol{J}$ is introduced as

$$\boldsymbol{J} = (\boldsymbol{f} - \boldsymbol{S}\boldsymbol{c})^T(\boldsymbol{f} - \boldsymbol{S}\boldsymbol{c}). \tag{23}$$

The coefficient vector $\boldsymbol{c}$ is determined through minimizing (23). The minimizing problem is expressed as

$$\frac{\partial \boldsymbol{J}}{\partial \boldsymbol{c}} = -2\left(\boldsymbol{S}^T\boldsymbol{f} - \boldsymbol{S}^T\boldsymbol{S}\boldsymbol{c}\right)$$
$$= 0. \tag{24}$$

Therefore, the solution of the least-squares problem (24) is calculated as

$$\boldsymbol{c} = \left(\boldsymbol{S}^T\boldsymbol{S}\right)^{-1}\boldsymbol{S}^T\boldsymbol{f}. \tag{25}$$

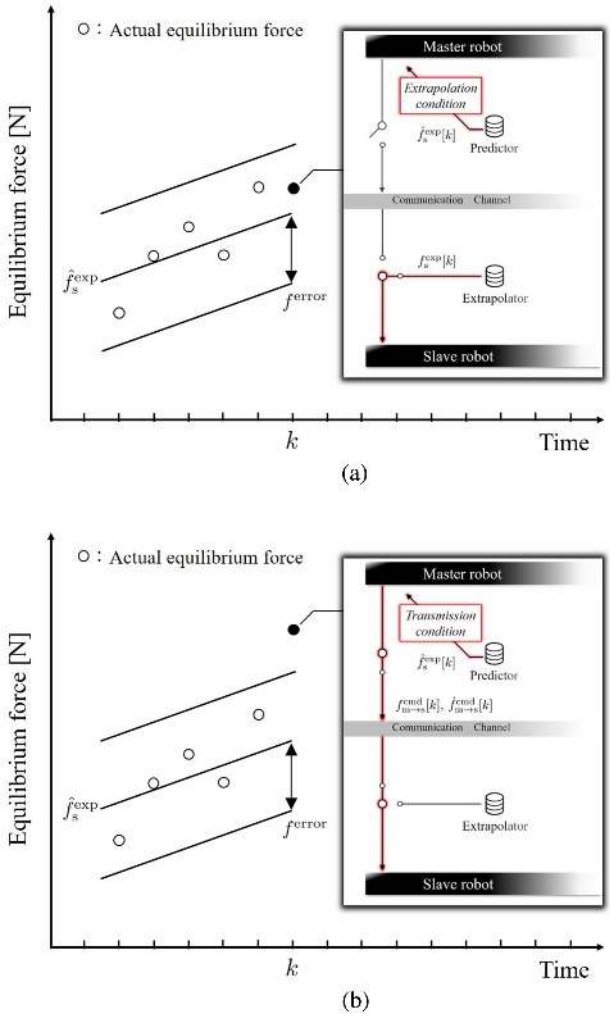

Fig. 4. Mode transition in proposed method. (a) Extrapolation mode. (b) Transmission mode.

By solving (25), the time derivative of $\hat{f}^{\mathrm{cmd}}_{m\to s}[k]$ is calculated as

$$\dot{\hat{f}}^{\mathrm{cmd}}_{m\to s}[k] = c_1. \tag{26}$$

IV. Simulations

Two types of simulations are shown in this section. The simulations were established in Section IV-C. In the first simulation in Section IV-A, the parameters in the proposed method were determined. In the second simulation in Section IV-B, the performance examinations were carried out with the different motion frequencies.

We simulated the motors and the environment object similar to the experimental setup shown in Fig. 5. Two linear motors were used as the master robot and the slave robot. The operator moved the master robot and the slave robot contacted with the aluminum block two times. In the contact motion, the operator pushed the block with 5.0 N. The simulated operator's motion is shown in Fig. 6. In the figure, the shaded area denotes the contact motion. Parameters are shown in Table II. Feedback gains were tuned by trial and error referring to the study by [19].

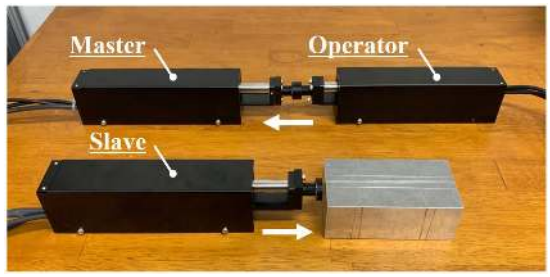

Fig. 5. Experimental setup.

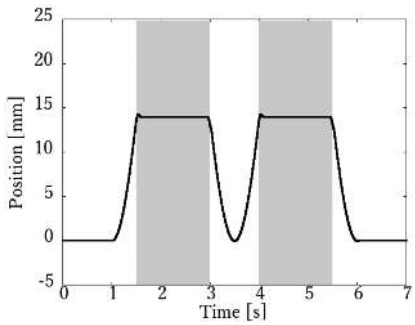

Fig. 6. Operator's motion in simulations (motion frequency : 0.4 Hz).

TABLE II
Parameters in Simulations and Experiments

Parameters	Definitions	Value
K_{p}	Positional feedback gain	2500 s^{-2}
K_{v}	Velocity feedback gain	100 s^{-1}
K_{f}	Force feedback gain	1.0 $\mathrm{m/Ns}^{-1}$
δt	Sampling time	0.2 ms
	Cutoff frequency of DOB	300 rad/s
	Cutoff frequency of RFOB	300 rad/s
	Motor mass	0.3 kg
	- Simulation -	
	Stiffness (human)	200 N/m
	Viscosity (human)	30 Ns/m
	Stiffness (environment)	5000 N/m
	Viscosity (environment)	100 Ns/m

Noise included in position sensing was simulated as a random Gaussian noise with mean 0 m and standard derivation 0.16 μm.

A. Validation of Parameters

In this section, the validity of the setting parameters was confirmed. The aforementioned contact motion was simulated, measuring the transmitted data size from the master side to the slave side. The compression ratio and the root mean square error (RMSE) of the force error between the two robots were compared using a different threshold of the pre-extrapolation f^{error}. The compression ratio was calculated using the transmitted data size of the conventional method that transmitted position, velocity, and force data. In the same procedure, the validity of the window size of the S–G filter n_{w} was confirmed.

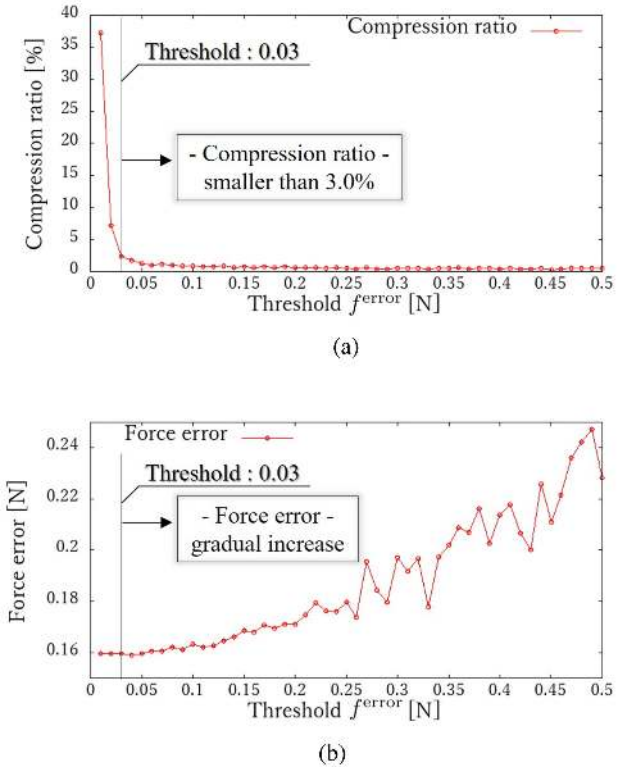

Fig. 7. Performance with different thresholds. (a) Compression ratio. (b) RMSE of force error.

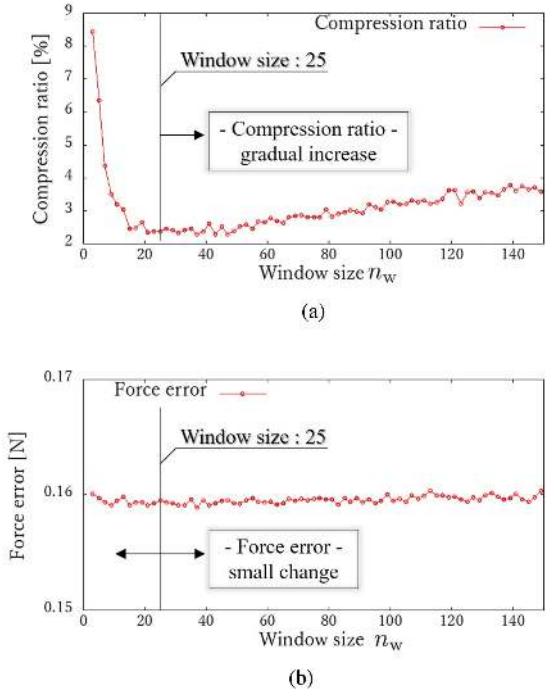

Fig. 8. Performance with different window sizes. (a) Compression ratio. (b) RMSE of force error.

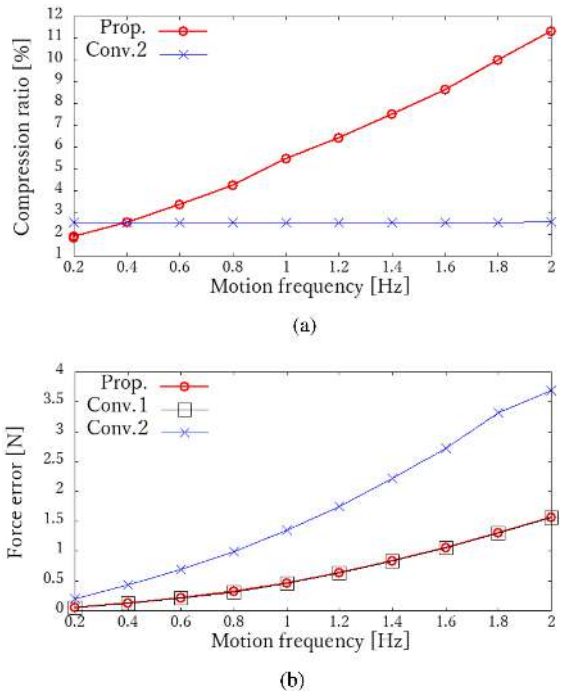

Fig. 9. Performance with different motion frequencies. (a) Compression ratio. (b) RMSE of force error.

Fig. 7(a) shows the compression ratio, and Fig. 7(b) shows the RMSE of the force error with different f^{error}. As shown in Fig. 7(a), the compression ratio was smaller than 3.0% if f^{error} was larger than 0.03 N. On the other hand, as shown in Fig. 7(b), the larger f^{error} became, the larger the force error between the two robots became. To expect the high traffic reduction effect, f^{error} should take a larger value than 0.03 N, while f^{error} should take a value as small as possible to avoid performance deterioration of haptic transmission. In this article, f^{error} was set to 0.03 N in Section IV-B and experiments.

Fig. 8(a) shows the compression ratio, and Fig. 8(b) shows the RMSE of the force error with different window sizes of S-G filter n_{w}. As shown in Fig. 8(a), if n_{w} was too small, the compression ratio became large. On the contrary, as n_{w} took larger value than 41, the compression ratio became gradually large. Therefore, n_{w} should take a value from 15 to 41. On the other hand, as shown in Fig. 8(b), the value of n_{w} did not produce a large effect on the RMSE based of the force error between the two robots. Therefore, the window size n_{w} was decided, considering the effect on the compression ratio's improvement. In Section IV-B and the experiments, n_{w} was set to 25.

B. Performance Examination With Different Motion Frequencies

The same indices used in the previous simulations were compared with different motion frequencies. Moreover, the same comparisons were carried out with two types of conventional four-channel bilateral control systems:

1) Conv. 1:
   a) The transmitted data were not compressed; thus, the packet transmission frequency was 5000 Hz, the same as the control frequency.
2) Conv. 2:
   a) The packet transmission frequency was reduced to 125 Hz.

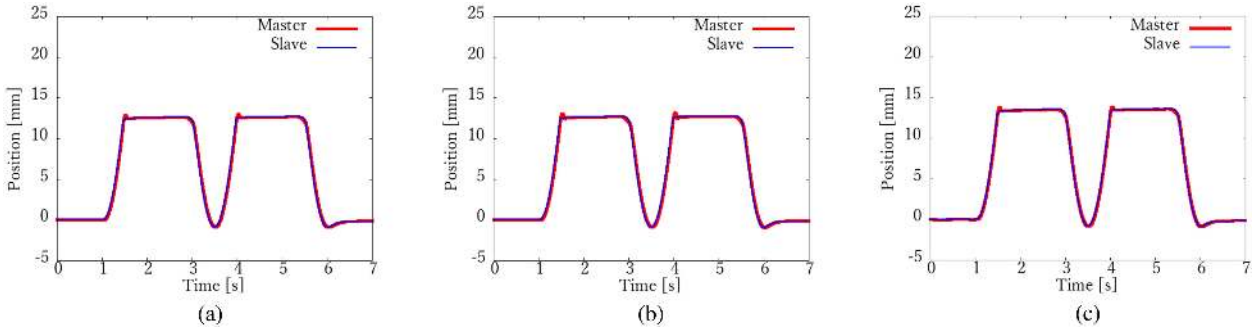

Fig. 10. Position responses in experiments (without time delay). (a) Conv. 1. (b) Conv. 2. (c) Proposed method.

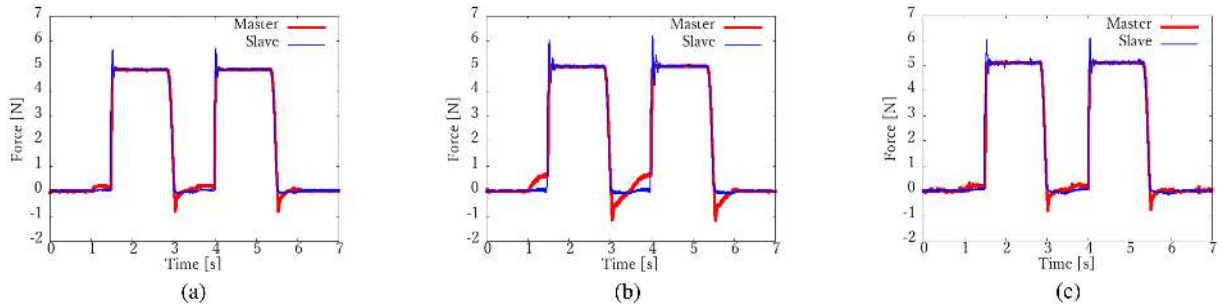

Fig. 11. Force responses in experiments (without time delay). (a) Conv. 1. (b) Conv. 2. (c) Proposed method.

In these conventional methods, position, velocity, and force data were transmitted.

Fig. 9(a) shows the compression ratio with different motion frequencies. As shown in the result, the compression ratio got increased in proportion to the operator's motion frequency, due to the difficulty of predicting rapid change of the equilibrium force. However, even in the worst case when motion frequency was set to 2.0 Hz, the compression ratio was less than 12%. Moreover, considering the human motion frequency is not so large in general, this result shows the effectiveness of the application of the proposed method.

Fig. 9(b) shows the RMSE of the force error with different motion frequencies. In common with the all three methods, the force error got large as the motion frequency increased due to the increase of the operational force on the master side. In particular, the Conv. 2 showed the worst performance affected by the reduced communication frequency. On the other hand, the proposed method showed the almost same performance with the Conv. 1, which had high communication frequency. This simulation result verifies that the proposed method does not degrade the haptic transmission performance of the conventional four-channel bilateral control system regardless of operator's motion frequency.

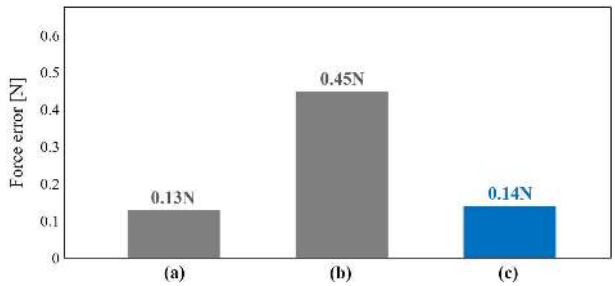

Fig. 12. RMSE of force error in experiments (3.1–3.9 s, without time delay). (a) Conv. 1. (b) Conv. 2. (c) Proposed method.

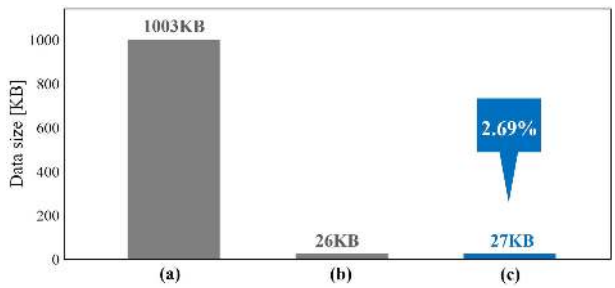

Fig. 13. Traffic reduction effect in experiments (without time delay). (a) Conv. 1. (b) Conv. 2. (c) Proposed method.

V. Experiments

A. Experimental Setup

The experimental setup is shownin Fig. 5. Two linear motors (L120Q: GMC Hillstone co., Ltd.) were used as the master and the slave robots. These two motors were controlled by different PCs and they were connected with a network emulator, which produced communication time delay. Positions of these motors were measured by the linear encoders (RGH24: RENISHAW plc.). The slave robot was contacted with an aluminum block.

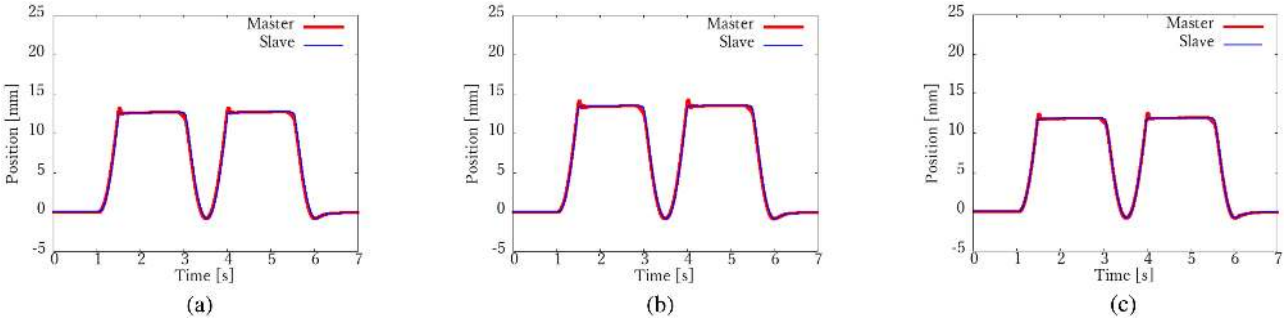

Fig. 14. Position responses in experiments (with time delay). (a) Conv. 1. (b) Conv. 2. (c) Proposed method.

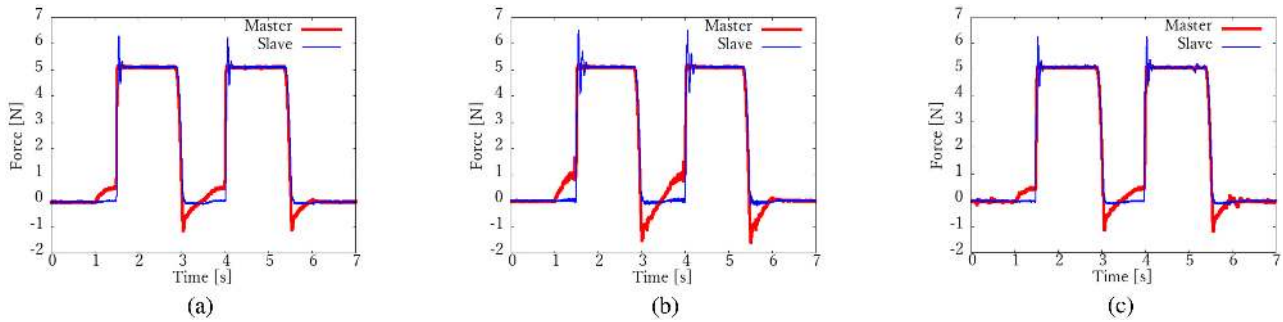

Fig. 15. Force responses in experiments (with time delay). (a) Conv. 1. (b) Conv. 2. (c) Proposed method.

Parameters used in the experiments were the same as the simulations and they are shown in Table II.

B. Experiments With/Without Communication Time Delay

First, experiments were conducted under no communication time delay and the results are shown in Figs. 10–13. The position and force responses are shown in Figs. 10 and 11, respectively. The force response of the master robot is plotted in the reverse value to compare with the slave side's one. As shown in the results, the contact motion was realized nevertheless the transmitted haptic data size was reduced by applying the proposed method. The most conspicuous difference in the responses of the three different methods was the force error in the free motion. The RMSE of the force error in free motion (3.1–3.9 s) was compared in Fig. 12. The proposed method offered the almost same force transmission performance in free motion with the one having the high packet transmission rate. The transmitted data size was summarized in Fig. 13. By applying the proposed method, the transmitted data size was reduced to 2.69% compared with the Conv. 1.

Second, the same experiments were conducted under 3.0 ms time delay. The results are shown in Figs. 14–17. The difference with the previous experimental results was the enlarged force error in the free motion induced by the communication time delay. Except for this force error that was summarized in Fig. 16, the proposed method showed the same effectiveness with the previous experimental results even under the communication time delay. The performance could be improved by implementing conventional methods that were utilized with the conventional four-channel bilateral control system [12][13].

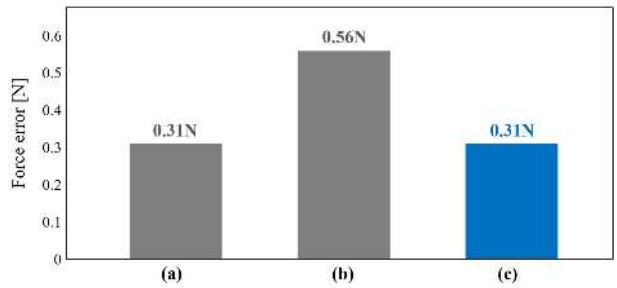

Fig. 16. RMSE of force error in experiments (3.1–3.9 s, with time delay). (a) Conv. 1. (b) Conv. 2. (c) Proposed method.

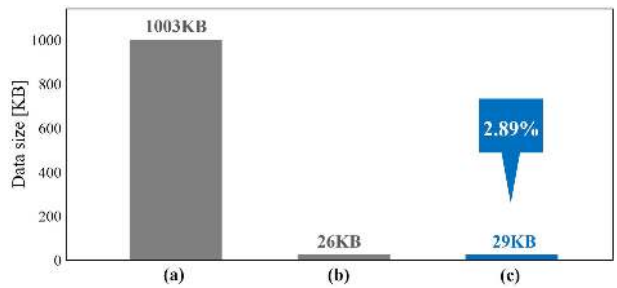

Fig. 17. Traffic reduction effect in experiments (with time delay). (a) Conv. 1. (b) Conv. 2. (c) Proposed method.

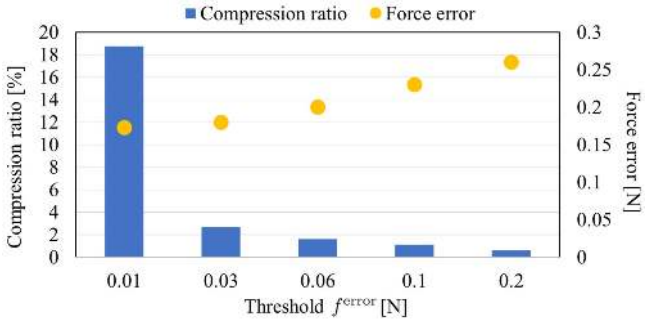

Fig. 18. Performance evaluation with different thresholds.

C. Performance Evaluation With Different Thresholds

Contact motion experiments were conducted in Section V-B with different thresholds f^{error} under no communication time delay. Experimental results are summarized in Fig. 18. As shown in the result, compression ratio and haptic transmission performance are in the relationship of tradeoff in the proposed method. In this article, the threshold f^{error} was designed to avoid increasing RMSE of force error, which led to a little conservative design. The traffic reduction effect is expected to be improved by designing the proposed method standing on the human perception as conducted in the literature for position or force communication [16]–[18]. The human perception-based investigation will provide novel insights since the proposed method applies equilibrium force communication, which has not been investigated well in the literature.

VI. Conclusion

In this article, we realized the prediction-based communication traffic reduction in the four-channel bilateral control system. By applying the proposed method, the transmit data size is reduced without losing the haptic transmission performance of the conventional four-channel bilateral control system. The setting parameters of the proposed method was determined through the simulation-based performance examinations. The effectiveness of the proposed method was verified by experiments. The experimental results also showed that the proposed method could be applied even under the communication time delay. The proposed method succeeded to reduce the transmitted data size less than 3.0%. The proposed method will expand the choice of networks that the high-performance bilateral control system could be realized.

As future works, detailed performance and stability analysis are expected to be conducted considering the effects of control gains or thresholds. Moreover, the proposed method should be investigated under more practical communication conditions such as time-varying delay or packet loss. These severe conditions are inevitable especially when wireless networks are utilized. As for performance evaluation, the proposed method should be evaluated through more practical tasks using a multidegrees-of-freedom experimental setup. From the performance, which was realized in the experiments, the proposed method is expected to expand its availability with a variety of tasks.

References

[1] K. Antonakoglou, X. Xu, E. Steinbach, T. Mahmoodi, and M. Dohler, "Toward haptic communications over the 5G tactile internet," *IEEE Commun. Surveys Tuts.*, vol. 20, no. 4, pp. 3034–3059, 4Q 2018.
[2] M. Aazam, K. A. Harras, and S. Zeadally, "Fog computing for 5g tactile industrial internet of things: QoE-aware resource allocation model," *IEEE Trans. Ind. Informat.*, vol. 15, no. 5, pp. 3085–3092, May 2019.
[3] T. Nozaki, T. Mizoguchi, Y. Saito, D. Yashiro, and K. Ohnishi, "Recognition of grasping motion based on modal space haptic information using DP pattern-matching algorithm," *IEEE Trans. Ind. Informat.*, vol. 9, no. 4, pp. 2043–2051, Nov. 2013.
[4] M. Condoluci, T. Mahmoodi, E. Steinbach, and M. Dohler, "Soft resource reservation for low-delayed teleoperation over mobile networks," *IEEE Access*, vol. 5, pp. 10445–10455, 2017.
[5] A. Aijaz, "Toward human-in-the-loop mobile networks: A radio resource allocation perspective on haptic communications," *IEEE Trans. Wireless Commun.*, vol. 17, no. 7, pp. 4493–4508, Jul. 2018.
[6] D. A. Lawrence, "Stability and transparency in bilateral teleoperation," *IEEE Trans. Robot. Autom.*, vol. 9, no. 5, pp. 624–637, Oct. 1993.
[7] T. Nozaki, T. Mizoguchi, and K. Ohnishi, "Real-world haptics for motion realization," *IEEJ J. Ind. Appl.*, vol. 2, no. 1, pp. 1–6, Jan. 2013.
[8] A. Hace and M. Franc, "FPGA implementation of sliding-mode-control algorithm for scaled bilateral teleoperation," *IEEE Trans. Ind. Informat.*, vol. 9, no. 3, pp. 1291–1300, Aug. 2013.
[9] Y. Yuan, Y. Wang, and L. Guo, "Force reflecting control for bilateral teleoperation system under time-varying delays," *IEEE Trans. Ind. Informat.*, vol. 15, no. 2, pp. 1162–1172, Feb. 2019.
[10] D. Yashiro and K. Ohnishi, "Performance analysis of bilateral control system with communication bandwidth constraint," *IEEE Trans. Ind. Electron.*, vol. 58, no. 2, pp. 436–443, Feb. 2011.
[11] R. J. Anderson and M. W. Spong, "Bilateral control of teleoperators with time delay," *IEEE Trans. Autom. Control*, vol. 34, no. 5, pp. 494–501, May 1989.
[12] K. Natori, T. Tsuji, K. Ohnishi, A. Hace, and K. Jezernik, "Time-delay compensation by communication disturbance observer for bilateral teleoperation under time-varying delay," *IEEE Trans. Ind. Electron.*, vol. 57, no. 3, pp. 1050–1062, Mar. 2010.
[13] A. Suzuki and K. Ohnishi, "Frequency-domain damping design for time-delayed bilateral teleoperation system based on modal space analysis," *IEEE Trans. Ind. Electron.*, vol. 60, no. 1, pp. 177–190, Jan. 2013.
[14] N. Sakr, J. Zhou, N. D. Georganas, and J. Zhao, "Prediction-based haptic data reduction and transmission in telementoring systems," *IEEE Trans. Instrum. Meas.*, vol. 58, no. 5, pp. 1727–1736, May 2009.
[15] N. Sakr, N. D. Georganas, and J. Zhao, "Human perception-based data reduction for haptic communication in six-DoF telepresence systems," *IEEE Trans. Instrum. Meas.*, vol. 60, no. 11, pp. 3534–3546, Nov. 2011.
[16] P. Hinterseer, S. Hirche, S. Chaudhuri, E. Steinbach, and M. Buss, "Perception-based data reduction and transmission of haptic data in telepresence and teleaction systems," *IEEE Trans. Signal Process.*, vol. 56, no. 2, pp. 588–597, Feb. 2008.
[17] S. Hirche and M. Buss, "Human-oriented control for haptic teleoperation," *Proc. IEEE*, vol. 100, no. 3, pp. 623–647, Mar. 2012.
[18] W. Fu, A. Landman, M. M. van Paassen, and M. Mulder, "Modeling human difference threshold in perceiving mechanical properties from force," *IEEE Trans. Human-Mach. Syst.*, vol. 48, no. 4, pp. 359–368, Aug. 2018.
[19] W. Iida and K. Ohnishi, "Reproducibility and operationality in bilateral teleoperation," in *Proc. IEEE Int. Workshop AMC*, Mar. 2004, pp. 217–222.
[20] T. Nozaki, S. Shimizu, T. Murakami, and R. Oboe, "Impedance field expression of bilateral control for reducing data traffic in haptic transmission," *IEEE Trans. Ind. Electron.*, vol. 66, no. 2, pp. 1142–1150, Feb. 2019.
[21] K. Ohnishi, M. Shibata, and T. Murakami, "Motion control for advanced mechatronics," *IEEE/ASME Trans. Mechatronics*, vol. 1, no. 1, pp. 56–67, Mar. 1996.
[22] T. Murakami, F. Yu, and K. Ohnishi, "Torque sensorless control in multidegree-of-freedom manipulator," *IEEE Trans. Ind. Electron.*, vol. 40, no. 2, pp. 259–265, Apr. 1993.
[23] A. Savitzky and M. J. E. Golay, "Smoothing and differentiation of data by simplified least squares procedures," *Anal. Chem.*, vol. 36, pp. 1627–1639, Jul. 1964.

[24] R. W. Schafer, "What is a Savitzky–Golay filter?," *IEEE Signal Process. Mag.*, vol. 28, no. 4, pp. 111–117, Jul. 2011.
[25] M. U. A. Bromba and H. Ziegler, "Application hints for Savitzky–Golay smoothing filters," *Anal. Chem.*, vol. 53, no. 11, pp. 1583–1586, Sep. 1981.
[26] J. Luo, K. Ying, P. He, and J. Bai, "Properties of Savitzky–Golay digital differentiators," *Digit. Signal Process.*, vol. 15, no. 2, pp. 122–136, Mar. 2005.
[27] H. Kaneko and K. Funatsu, "Smoothing-combined soft sensors for noise reduction and improvement of predictive ability," *Ind. Eng. Chem. Res.*, vol. 54, no. 50, pp. 12 630–12 638, Dec. 2015.

Satoshi Hangai (Student Member, IEEE) received the B.E. degree in system design engineering and the M.E. degrees in integrated design engineering from Keio University, Yokohama, Japan, in 2018, and 2020, respectively.

He is currently with Nippon Steel Corporation. His research interests include haptics and motion control.

Takahiro Nozaki (Member, IEEE) received the B.E. degree in system design engineering and the M.E. and Ph.D. degrees in integrated design engineering from Keio University, Yokohama, Japan, in 2010, 2012, and 2014, respectively.

In 2014, he joined Yokohama National University, Yokohama, Japan, as a Research Associate. In 2015, he joined the Department of System Design Engineering, Keio University, where he is currently an Assistant Professor. He is with the Massachusetts Institute of Technology, Cambridge, MA, USA, as a Visiting Researcher.